Skeletor, a Novel Chromosomal Protein That Redistributes during Mitosis Provides Evidence for the Formation of a Spindle Matrix

Diana L. Walker, Dong Wang, Ye Jin, Uttama Rath, Yanming Wang, Jørgen Johansen, and Kristen M. Johansen

Department of Zoology and Genetics, Iowa State University, Ames, Iowa 50011

Abstract. A spindle matrix has been proposed to help organize and stabilize the microtubule spindle during mitosis, though molecular evidence corroborating its existence has been elusive. In *Drosophila*, we have cloned and characterized a novel nuclear protein, skeletor, that we propose is part of a macromolecular complex forming such a spindle matrix. Skeletor antibody staining shows that skeletor is associated with the chromosomes at interphase, but redistributes into a true fusiform spindle structure at prophase, which precedes microtubule spindle formation. During metaphase, the spindle, defined by skeletor antibody labeling, and the microtubule spindles are coaligned. We find that the skeletor-defined spindle maintains its fusiform spindle structure from end to end across the metaphase plate during anaphase when the chromosomes segregate. Consequently, the properties of the skeletor-defined spindle make it an ideal substrate for providing structural support stabilizing microtubules and counterbalancing force production. Furthermore, skeletor metaphase spindles persist in the absence of microtubule spindles, strongly implying that the existence of the skeletor-defined spindle does not require polymerized microtubules. Thus, the identification and characterization of skeletor represents the first direct molecular evidence for the existence of a complete spindle matrix that forms within the nucleus before microtubule spindle formation.

Key words: spindle matrix • mitosis • chromosomes • microtubules • *Drosophila*

Introduction

The formation of a mitotic spindle apparatus is essential for cell division to occur. Major structural components of the spindle apparatus include tubulin and its associated motor proteins that are recruited from the cytoplasm. However, recent studies have suggested that nuclear components, including chromosome-associated elements, may also play an important role in spindle apparatus assembly and function. For example, rupture of the nuclear envelope during prophase that prematurely exposed centrosomes and microtubules to the chromosomes, and other nuclear contents, induced rapid spindle assembly (Zhang and Nicklas, 1995a). In contrast, assembly of microtubules was completely inhibited if the nucleus was mechanically removed from a late prophase cell (Zhang and Nicklas, 1995b). In female meiotic cells, in the absence of centrosomes, microtubules nucleated around chromosomes and then self-organized into a bipolar spindle (Gard, 1992; Theurkauf and Hawley, 1992). Various nuclear molecules have been directly shown to undergo a mitosis-specific redistribution pattern and associate with microtubules and centrosomes, including the centromere proteins (CENPs) (Pankov et al., 1990; Yen et al., 1991; Casiano et al., 1993), the inner centromere proteins (INCENPs) (Cooke et al., 1987; Earnshaw and Cooke, 1991; Mackay et al., 1993), and the nuclear mitotic apparatus (NuMA) proteins (Lydersen and Pettijohn, 1980; Compton et al., 1992; Yang and Snyder, 1992). Furthermore, the discovery of microtubule flux at both ends of spindle microtubules (Mitchison, 1989; Sawin and Mitchison, 1991, 1994), in conjunction with the demonstration that chromosomes whose kinetochore fibers have been severed by UV-microbeam irradiation still moved poleward (Forer et al., 1997), suggest that current models for how chromosomes move to the poles are incomplete and that additional structural components of the spindle apparatus may exist (for review see Pickett-Heaps et al., 1997). This notion is supported by studies in which preparations of "spindle remnants" revealed that kinesin associates with a nonmicrotubule component of the spindle (Leslie et al., 1987). Thus, these observations have led to the proposal of the existence of a "spindle matrix" involved in stabilizing and organizing the microtu-

The online version of this article contains supplemental material.

Address correspondence to Kristen M. Johansen, Department of Zoology and Genetics, 3154 Molecular Biology Building, Iowa State University, Ames, IA 50011. Tel.: (515) 294-7959. Fax: (515) 294-4858. E-mail: kristen@iastate.edu

bule spindle (for review see Pickett-Heaps et al., 1997). However, direct molecular evidence for such a spindle matrix has been elusive.

Here, we have used the monoclonal antibody 2A (mAb2A) to identify a novel nuclear protein that is localized in *Drosophila* nuclei in a striking cell cycle–specific pattern (Johansen, 1996; Johansen et al., 1996), which we have named skeletor. Antibodies specifically generated against skeletor show that it is associated with the chromosomes at interphase, but redistributes into a spindle-like structure at prophase that precedes microtubule spindle formation. During metaphase, the spindle defined by skeletor antibody labeling and the microtubule spindles are coaligned. Skeletor metaphase spindles persisted in the absence of microtubule spindles, as they were still intact after microtubule depolymerization by nocodazole or low temperature treatment. Thus, these findings suggest that skeletor is a chromosome-derived protein that reorganizes during mitosis to participate in the formation of a structure exhibiting the features of a spindle matrix.

Materials and Methods

Drosophila Stocks

Wild-type Oregon-R fly stocks were maintained according to standard protocols (Roberts, 1986).

Molecular Cloning and Sequence Analysis

Genomic and cDNA library screenings were performed using standard procedures (Sambrook et al., 1989). mAb2A was used to screen a λgt11 library containing genomic sequence (Goldstein et al., 1986), and a skeletor-positive clone was identified. This clone was used to isolate overlapping clones from oligo-dT primed (a gift from Dr. P. Hurban, Paradigm Genetics, Inc., Research Triangle Park, NC) and random primed (CLONTECH Laboratories, Inc.) embryonic cDNA libraries, both in λgt10. Three expressed sequence tagged clones with homology to this region were also identified, two from a larval library and one from an adult head library (LP06211, LP09436, and GH12580, respectively; Research Genetics, Inc.). The original skeletor-positive clone was also used to isolate a genomic clone containing the complete locus from a Canton-S library in λEMBL3 (a gift of Dr. I. Dawson, Yale University, New Haven, CT). DNA sequencing was performed at the Iowa State University DNA Sequencing and Synthesis Facility. Skeletor sequence was compared with known and predicted sequences using the National Center for Biotechnology Information BLAST server. The sequence was further analyzed using PSORT II algorithms to predict subcellular localization and putative nuclear localization signals (Robbins et al., 1991; Reinhardt and Hubbard, 1998).

Antibody Generation

Residues 552–668 of the predicted skeletor protein were subcloned using standard techniques (Sambrook et al., 1989) into pGEX-3 (Amersham Pharmacia Biotech) to generate the construct 3gexF. The correct orientation and reading frame of the insert was verified by sequencing. 3gexF–GST fusion protein was expressed in XL1-Blue cells (Stratagene) and purified over a glutathione agarose column (Sigma-Aldrich), according to the pGEX manufacturer's instructions (Amersham Pharmacia Biotech). The purified fusion protein was used to generate polyclonal antibodies in the rabbit Freja using standard procedures (Harlow and Lane, 1988). Affinity purification of antibodies was performed using positive and negative affinity columns as per the manufacturer's instructions (Amersham Pharmacia Biotech). The mAb1A1 was generated by injection of 50 μg of 3gexF into BALB/c mice at 21 d intervals. After the third boost, mouse spleen cells were fused with Sp2 myeloma cells and a monospecific hybridoma line was established and used to generate ascites fluid using standard procedures (Harlow and Lane, 1988). The mAb1A1 is of the IgM subtype.

A synthetic peptide containing residues 497–511 (KPTLDELFAEDINEEE) of skeletor was synthesized (Quality Controlled Biochemicals) with an added cysteine residue at its NH_2 terminus for coupling purposes and covalently coupled to keyhole limpet hemocyanin (Pierce Chemical Co.) carrier protein with sulfosuccinimidyl 4-(*N*-maleimidomethyl) cyclohexane-1-carboxylate, as per the manufacturer's instructions (Pierce Chemical Co.). Conjugated peptide was used to generate the polyclonal Bashful antiserum in rabbits and the mAb1D4 in mice, as described above. Polyclonal antibodies were affinity purified, as described above, except that positive selection columns contained peptide and negative selection columns contained keyhole limpet hemocyanin coupled to Sepharose 4B. The mAb1D4 is of the IgM subtype.

The ORF1 fusion protein was constructed by PCR, amplifying the fragment between cDNA bases 391–1175 using Vent polymerase (New England Biolabs, Inc.) and gene-specific primers, according to the manufacturer's instructions and cloned inframe into the pGEX4T-1 vector (Amersham Pharmacia Biotech), generating a 57-kD GST-fusion protein containing sequences included in both ORF1a and ORF1b. The resulting construct was sequenced to confirm its fidelity. This fusion protein was purified over a glutathione agarose column and used to generate the mAb6A6, as described above. All procedures for mAb and ascites production were performed by the Iowa State University Hybridoma Facility.

Northern and Western Blot Analysis

$PolyA^+$ mRNA was purified from 0 to 15 h embryos using the FastTrack kit (Invitrogen), and 20 μg of $polyA^+$ mRNA was fractionated on 1.2% agarose formaldehyde gels, transferred to nitrocellulose, and hybridized with the addition of dextran sulfate (10%), according to standard protocols (Sambrook et al., 1989). Skeletor-specific probes were generated by purifying cDNA subclone fragments from either the first 720 bp (the 5′ probe) or bp 4,077–4,427 (3′ probe) of the skeletor transcript using GeneClean (Bio 101) and synthesizing random primer ^{32}P-labeled probe using the Prime-A-Gene kit (Promega), according to manufacturer's instructions. High stringency hybridization and washing conditions were employed (Sambrook et al., 1989).

Protein extracts were prepared from dechorionated embryos homogenized in lysis buffer (0.137 M NaCl, 20 mM Tris-HCl, pH 8.0, 10% glycerol, 1% NP-40). Protease inhibitors were routinely added to the homogenization buffers. Proteins were separated on SDS-PAGE gels and transferred to nitrocellulose, and incubated with Freja or Bashful antibody overnight, washed in TBS (0.9% NaCl, 100 mM Tris-HCl, pH 7.5), incubated with HRP-conjugated goat anti–rabbit antibody (1:3,000) (Bio-Rad Laboratories) for 2.5 h, washed in TBS, and the antibody complex was visualized by incubation in 0.2 mg/ml DAB/0.03% H_2O_2/0.0008% $NiCl_2$ in TBS. Nuclear preparations were performed according to Elgin and Hood (1973). Essentially, frozen embryos were thawed into 10 volumes of buffer A (50 mM Tris-HCl, pH 7.5, 50 mM NaCl, 5 mM $MgCl_2$, 250 mM sucrose), Dounce homogenized four strokes with a tight pestle, filtered through two layers of 120-μm mesh, and centrifuged at 1,000 *g* for 10 min. The pellet was resuspended in five volumes of buffer A and centrifuged at 1,000 *g* for 10 min two additional times, yielding a purified nuclear pellet. All steps were performed at 0–4°C.

For immunoprecipitation experiments, 1 μg affinity purified Freja or Bashful antibodies were coupled with 5 μl protein G–Sepharose beads (Amersham Pharmacia Biotech) for 4 h at 4°C on a rotating wheel in 200 μl immunoprecipitation buffer (25 mM Tris-HCl, pH 7.5, 125 mM NaCl, 5 mM EDTA, 1% Triton X-100, 0.25% Sarkosyl, 0.25% sodium deoxycholate). Dechorionated embryos were homogenized on ice in immunoprecipitation buffer (200 embryos/100 μl immunoprecipitation buffer) and precleared with 5 μl normal sera and 20 μl protein G beads for 3 h at 4°C. The precleared lysate and protein G beads preloaded with the appropriate antibody were combined and incubated overnight at 4°C with continuous mixing. Beads were then washed three times for 15 min each with 1 ml of immunoprecipitation buffer. The resulting immunocomplexes were analyzed by SDS-PAGE and Western blotted according to standard techniques (Towbin et al., 1979), as described above.

Immunohistochemistry

Antibody labelings were performed as described previously (Johansen et al., 1996). For nuclear antibody-labeling studies, embryos (0–3 h) were dechorionated in a 50% Chlorox solution, washed with 0.7 M NaCl/0.2% Triton X-100, and fixed in a 1:1 heptane/fixative mixture for 20 min with vigorous shaking at room temperature. The fixative was either 4% paraformaldehyde in PBS or Bouin's fluid (0.66% picric acid, 9.5% formalin, 4.7% acetic acid). Vitelline membranes were then removed by shaking embryos in heptane/methanol (Mitchison and Sedat, 1983) at

room temperature for 30 s. Using epifluorescence, triple and quadruple labelings were performed with antibodies against skeletor, described above (rabbit sera or mouse IgM), anti–α-tubulin mouse IgG_1 antibody (Sigma-Aldrich) or anti-lamin rabbit antibody (a gift from Dr. P. Fisher, SUNY Stony Brook, Stony Brook, NY) and Hoechst to visualize the DNA. The appropriate TRITC-, FITC-, and Cy5-conjugated secondary antibodies (ICN Biomedicals or Jackson ImmunoResearch Laboratories) were used (1:200 dilution) to visualize primary antibody labeling. Confocal microscopy was performed with a Leica confocal TCS NT microscope system equipped with separate Argon-UV, Argon, Krypton, and HeNe lasers and the appropriate filter sets for Hoechst, FITC, TRITC, and Cy5 imaging. A separate series of confocal images for each fluorophor of double-labeled preparations were obtained simultaneously with z intervals of typically 0.5 μm. Images from the stacks were imported into Adobe® Photoshop where they were pseudocolored, image processed, and merged. Polytene chromosome squash preparations from late third instar larvae were immunostained by the skeletor antibody mAb1A1 essentially as described previously by Zink and Paro (1989) and Jin et al. (1999).

Perturbation Experiments

Dechorionated embryos from 0 to 3 h collections were added to heptane/PBS containing 10 μM nocodazole and shaken for 1 min, before adding fixative and incubating for an additional 20 min. Immunolabeling was performed as described above using Hoechst staining of DNA with anti-skeletor and anti–α-tubulin antibodies detected with TRITC-conjugated anti–mouse IgM- and FITC-conjugated anti–mouse IgG_1–specific secondary antibodies, respectively. Cold-treated embryos were incubated 1 min with prechilled heptane, transferred to prechilled PBS/0.1% Triton X-100, and rotated at 4°C for 15 min, transferred to cold heptane/Bouin's fluid and shaken for 30 s, rotated at 4°C for 20 min, and then processed for immunohistochemistry, as described above.

For antibody perturbation experiments, antibody injection into 0 to 30-min syncytial embryos followed the procedures of Baek and Ambrosio (1995), except that embryos were aligned for lateral microinjection. Approximately 1 nl of either mAb1A1 or a control ascites fluid, both of which had been precleared by centrifugation, was injected into each embryo. The control ascites fluid was derived from the commercially available MOPC-104E mineral oil–induced tumor cell line (ICN Biomedicals), which produces mouse IgM antibody and has the normal ascites fluid content of other mouse immunoglobulin and serum proteins, or from ascites fluid generated within our laboratory against the leech antigen lan3-2 (Huang et al., 1997) that does not cross react in *Drosophila*. Embryos were allowed to develop for 2.5 h at 20°C, after which they were fixed in Bouin's fluid, hand devitellinized with a tungsten needle, and stained with Hoechst, as described above, to observe the nuclear DNA staining patterns. Egg collections were routinely divided into two samples to be used for either experimental or control injections to minimize variability between egg samples. Embryos were mounted in glycerol with 5% *n*-propyl gallate, viewed under epifluorescence as described above, and scored blind as either wild-type, perturbed, or unfertilized. To test whether the difference in the distribution into these categories of experimental and control embryos was statistically significant, we performed a χ^2-test of the null hypothesis that the two distributions were different.

Online Supplemental Material

Quicktime movies of dynamic three-dimensional reconstructions of fluorescent images of nuclei in various stages of the cell cycle labeled with skeletor and/or tubulin antibody and with Hoechst accompanying Fig. 4 are available at http://www.jcb.org/cgi/content/full/151/7/1401/DC1.

Results

Molecular Cloning and Characterization of Skeletor

The mAb2A, which was previously shown to exhibit a dynamic nuclear staining pattern comprising a fibrous meshwork at interphase that redistributes to a spindle at metaphase (Johansen, 1996; Johansen et al., 1996), was used to screen a λgt11 genomic *Drosophila* expression library. A partial clone with a single ORF was identified and new antibodies, including the polyclonal sera Freja and the mAb1A1, were raised against a GST-fusion protein containing this sequence. The newly generated antibodies were used to stain early embryos, and a similar staining pattern to the original mAb2A staining pattern (compare with Figure 2 in Johansen et al., 1996) was observed (Fig. 1), strongly suggesting that an antigen contributing to the mAb2A staining pattern had been identified. Whereas the Freja antiserum and mAb1A1 have identical staining patterns, the labeling of mAb1A1 is considerably more robust wherever this antibody is used for the immunocytochemical-labeling studies. At interphase mAb1A1 stains a fibrous meshwork extending throughout the nucleus (Fig. 1 A), but as the nucleus enters prophase (Fig. 1 B), the staining begins to realign in a spindle-like pattern that becomes prominent by late prophase (Fig. 1 C). During prophase through late prometaphase, mAb1A1 labeling also appears to be associated with the nuclear envelope (Fig. 1, B–D). At metaphase and anaphase, mAb1A1 labels a spindle-like structure throughout its entire length (Fig. 1, E and F). During telophase, the mAb1A1 staining begins to segregate into the two daughter nuclei, reassuming its fibrous meshwork interphase appearance (Fig. 1, G and H) as the chromosomes begin to decondense. Based on this nuclear structural reorganization during mitosis as reflected by the mAb1A1 and Freja immunocytochemical labeling, we have named the antigen identified by these antibodies skeletor.

The skeletor fragment identified in the expression library screen was used to screen several cDNA libraries from which we obtained overlapping clones representing the complete skeletor cDNA sequence. Analysis of the cDNA sequence, as well as Northern blot analysis, show skeletor to be part of a complex locus (Fig. 2) and that alternative splicing gives rise to two mRNAs of 6.5 and 1.6 kb (Fig. 2, A and C). The larger of these mRNAs has bicistronic coding potential and spans a genomic region of ~10 kb. The 5′ region of ORF1 is included in both the larger and the smaller transcripts, but read through of a donor splice site in exon three in the shorter mRNA introduces 14 novel amino acids, an early stop codon, and an early polyadenylation signal (Fig. 2 A). This is schematically depicted as ORF1a (Fig. 2 B), which conceptually translates to yield a 32-kD protein. ORF1b in the longer transcript does not contain this stop codon, but extends to a stop codon in exon 7, thus predicting an 85-kD protein (Fig. 2 B). The overlapping ORF2 region (Fig. 2 B) contains the sequence originally identified by the mAb2A and predicts a protein of ~81 kD that corresponds to the skeletor product. Although searches of current databases reveal no obvious significant homologies or motifs to any previously described proteins, there are several notable features about the skeletor sequence. Analysis of the skeletor ORF using PSORT II algorithms, which discriminate between cytoplasmic or nuclear protein localization (Reinhardt and Hubbard, 1998), predict nuclear localization for skeletor with a score of 94.1%, in addition to the presence of a bipartite nuclear localization signal (Robbins et al., 1991) just downstream from the beginning of the predicted ORF2 (Fig. 2 F, boxed region). The overall sequence is proline rich, containing 12.7% proline distributed throughout the protein. Moreover, there are several low complexity regions, including a histidine-rich domain (Fig. 2 F, underlined) and a serine-rich region (Fig. 2 F, stippled box).

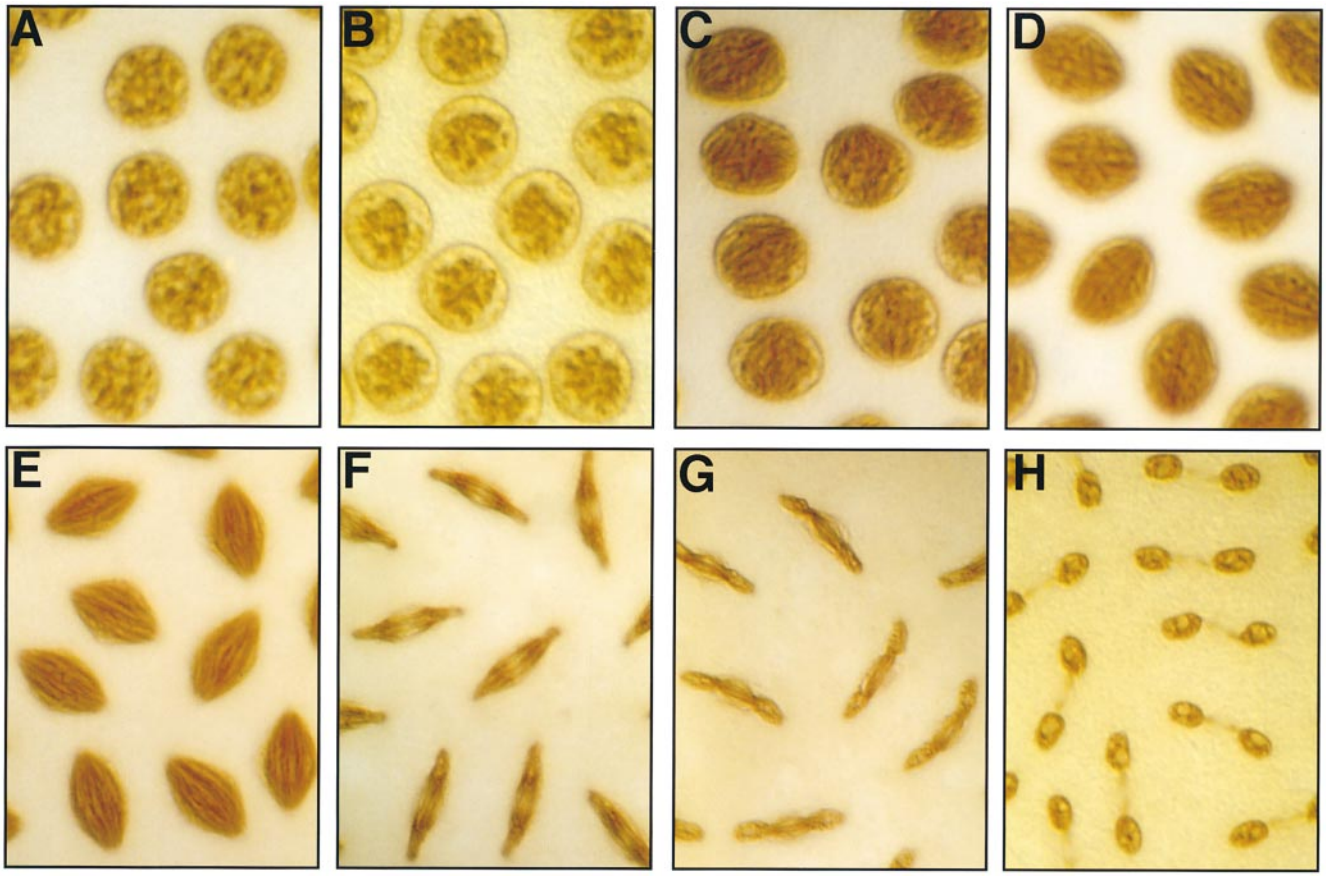

Figure 1. Drosophila embryo nuclei labeled by the skeletor mAb1A1 from various stages of the cell cycle. (A) interphase; (B) prophase; (C) late prophase; (D) prometaphase; (E) metaphase; (F) late anaphase; (G) early telophase; and (H) late telophase. At prophase (B), the interconnected meshwork, which was labeled with mAb1A1 in interphase (A), begins to undergo a condensation and reorientation that leads to the labeling of a spindle-like scaffold from late prophase (C) through anaphase (F). During interphase (A) and prophase (B and C), mAb1A1 labeling appears to be also associated with the nuclear envelope. The micrographs are Nomarski images of mAb1A1 labelings visualized using HRP-conjugated secondary antibody.

To further analyze the expression of the protein products from the skeletor region, additional antibodies were generated against the ORF1 NH_2-terminal sequence (mAb6A6), as well as against a synthetic peptide included within the skeletor ORF2 (mAb1D4 and the Bashful antiserum), but upstream from the original fragment recognized by mAb2A, mAb1A1, and the Freja antiserum (Fig. 2 B). As shown by Western blot analysis (Fig. 2 D), a protein of 32 kD corresponding to the ORF1a-encoded product is recognized by mAb6A6. However, we have not detected a protein of the predicted size of the ORF1b product in Western blots of embryonic protein extracts. Consequently, it is possible that its expression may be developmentally regulated and/or only appear in certain tissues at specific stages. The affinity purified Freja and Bashful antisera that were raised against two different regions of the skeletor ORF2 both detect an 81-kD product, as predicted for the protein size from this ORF. Cross-immunoprecipitation experiments further demonstrated that the 81-kD protein can be immunoprecipitated by either Bashful or Freja antibodies and detected on Western blots by the Bashful antiserum (Fig. 2 E). Unfortunately, both mAb1A1 and mAb1D4 are of the IgM subtype and do not show labeling on Western blots. Whereas mAb6A6 labels a cytoplasmically located antigen, mAb1D4 and the Bashful antiserum show an identical staining pattern to that observed with the mAb1A1 (data not shown), providing further evidence that the skeletor ORF2 is translated despite its unusual downstream position in the mRNA. However, the translation of the skeletor ORF2 appears to have additional unconventional features. Fig. 2 F shows the ORF2 cDNA sequence derived from the long RNA transcript (mRNA 2), along with the conceptual translation of ORF2 beginning at an ATG that is consistent with the 81-kD size detected on Western blots (Fig. 2, D and E). However, an inframe stop codon appears only nine codons downstream from the starting ATG, and there is no alternative ATG from which to initiate skeletor translation until 362 residues downstream. This inframe stop codon has been confirmed in five independent cDNAs from an embryonic library as well as an adult head cDNA clone from the Berkeley *Drosophila* genome project. This stop codon sequence was also found in sequence from a λEMBL3 genomic library, as well as in the recently deposited *Drosophila* genome project complete genomic sequence (Adams et al., 2000). However, the detection of the skeletor product with multiple antibodies generated against different protein domains shows that despite its unusual position downstream in the mRNA and its likely unconventional method of translation initiation, skeletor ORF2 is, in fact,

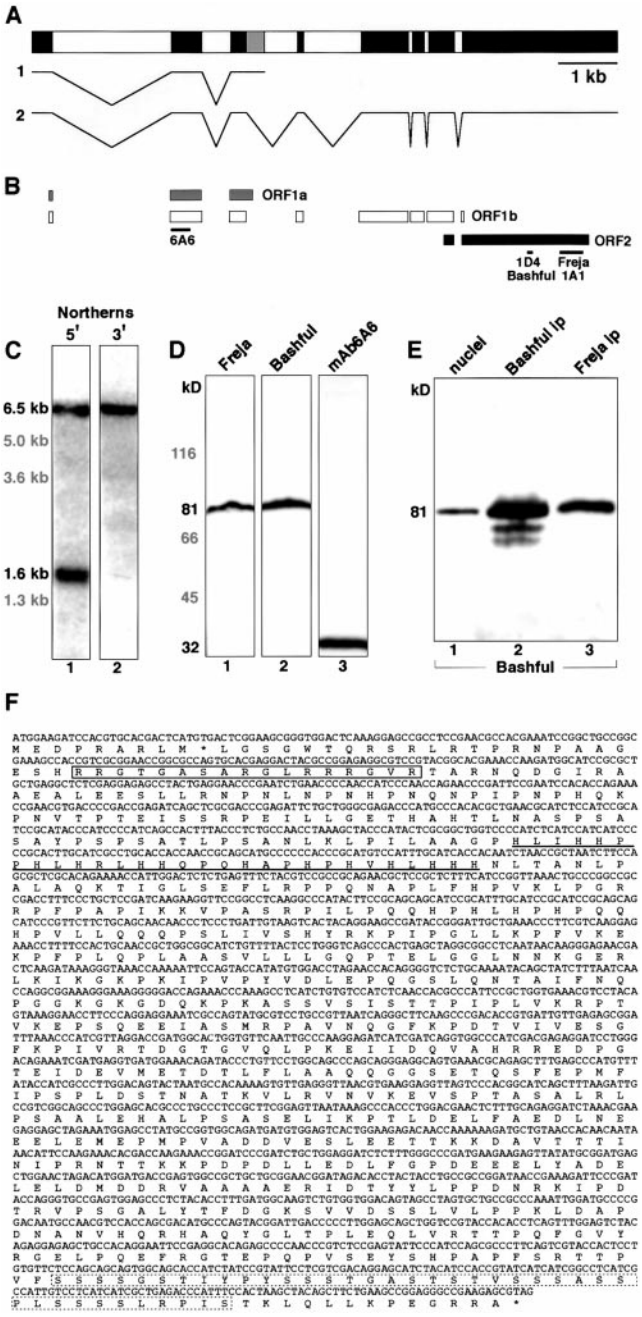

Figure 2. The organization and protein coding potential of the skeletor locus. (A) Diagram of the skeletor genomic locus. Sequencing of genomic and cDNA clones reveals that the skeletor locus gives rise to alternatively spliced products (1 and 2), which share their first and second exons (black regions), but diverge within the third (gray region). mRNA 1 fails to use a 5′-splicing donor signal used in mRNA 2, resulting in inclusion of sequences encoding a stop signal and a polyadenylation signal, thus generating a truncated 1.6-kb mRNA. The splicing pattern in mRNA 2 removes these signals, and, instead, incorporates an additional five exons, yielding a longer 6.5-kb mRNA product. (B) Diagram of the potential ORFs within the skeletor cDNAs. The protein coding potential of mRNA 1 is schematically depicted as ORF1a, drawn as gray boxes aligned beneath the appropriate regions shown in A. mRNA 2 includes two potential ORFs: ORF1b (white boxes), which differs from ORF1a at the alternative splice site, and ORF2 (black boxes), which is further downstream. New antibodies have been raised against the regions indicated (6A6, 1D4, and 1A1 are mAbs; Bashful and Freja are polyclonal antibodies). (C) Northern blot analysis reveals two alternatively spliced transcripts of 6.5 and 1.6 kb when probed with a 5′ probe (lane 1), but only the 6.5-kb mRNA when probed with a 3′ probe (lane 2). (D) Western blot analysis of embryonic protein extract shows that both Freja (lane 1) and Bashful (lane 2) recognize an 81-kD protein, consistent with an ORF2 product, wheras mAb6A6 recognizes a 32-kD protein (lane 3), consistent with the ORF1a product. (E) Immunoblots of extracts from embryonic nuclear fractions immunoblotted with Bashful and Freja skeletor antisera. Bashful antiserum recognizes the 81-kD skeletor band both in the nuclear fractions (lane 1) and after immunoprecipitation with Bashful (lane 2) and Freja (lane 3) antisera. (F) The predicted sequence for skeletor based on translation of mRNA 2. The nucleotide sequence within mRNA 2 corresponding to skeletor ORF2 is shown together with the putative translation. The predicted skeletor protein consists of 744 residues with an estimated molecular mass of 81 kD if translation is initiated at the indicated methionine. However, it should be noted that this methionine is followed by an inframe stop codon, and the exact mechanism of translation for this ORF is not known. The predicted sequence for the skeletor protein contains a bipartite nuclear localization signal (boxed), a histidine-rich region (underlined), and a serine-rich region (stippled box). This sequence data for mRNA 2 is available from GenBank/EMBL/DDBJ under accession no. AF321289. The nucleotide sequence for mRNA 1 is available from GenBank/EMBL/DDBJ under accession no. AF321290.

translated. This was further confirmed by the detection of a COOH-terminal V5 epitope tag added to ORF2 within the context of the complete mRNA 2 after expression in the S2 cell line (Walker, D.L., unpublished results).

Skeletor Reorganizes from the Chromosomes to a Spindle-like Structure during Mitosis

The distribution of skeletor during the cell cycle (Fig. 1) revealed a staining pattern at interphase that was reminiscent of chromosomal DNA labeling by Hoechst, suggesting that skeletor may associate with the chromosomes at interphase. Confocal analysis of interphase embryonic nuclei double labeled with anti-skeletor antibody (Fig. 3 A) and Hoechst to visualize the DNA (Fig. 3 B) confirmed a very high degree of overlap between skeletor labeling and chromosomal DNA (Fig. 3 C). To further verify this relationship, we directly double labeled *Drosophila* larval polytene chromosome squashes with anti-skeletor antibody and Hoechst. Fig. 3, D and E, shows that skeletor is localized to the polytene chromosomes in a pattern largely corresponding to that of the Hoechst labeling of chromosomal DNA. These data strongly indicate that skeletor is associated with the chromosomes at interphase. However, at metaphase, skeletor is clearly dissociated from the chromosomes and instead comprises part of a spindle-like structure (Fig. 3 G) that is coextensive with the microtubule mitotic spindle, except for the centrosomal regions (Fig. 3, H and I). From here on, this structure will be referred to as the skeletor spindle.

An interesting issue derived from these findings concerns the relative timing of skeletor-defined spindle formation with respect to microtubule spindle assembly. To address this question, we performed confocal analysis of double- and triple-labeled embryos at various stages in the mitotic cycle using either anti-skeletor and anti-tubulin antibodies or anti-skeletor and anti-lamin antibodies to-

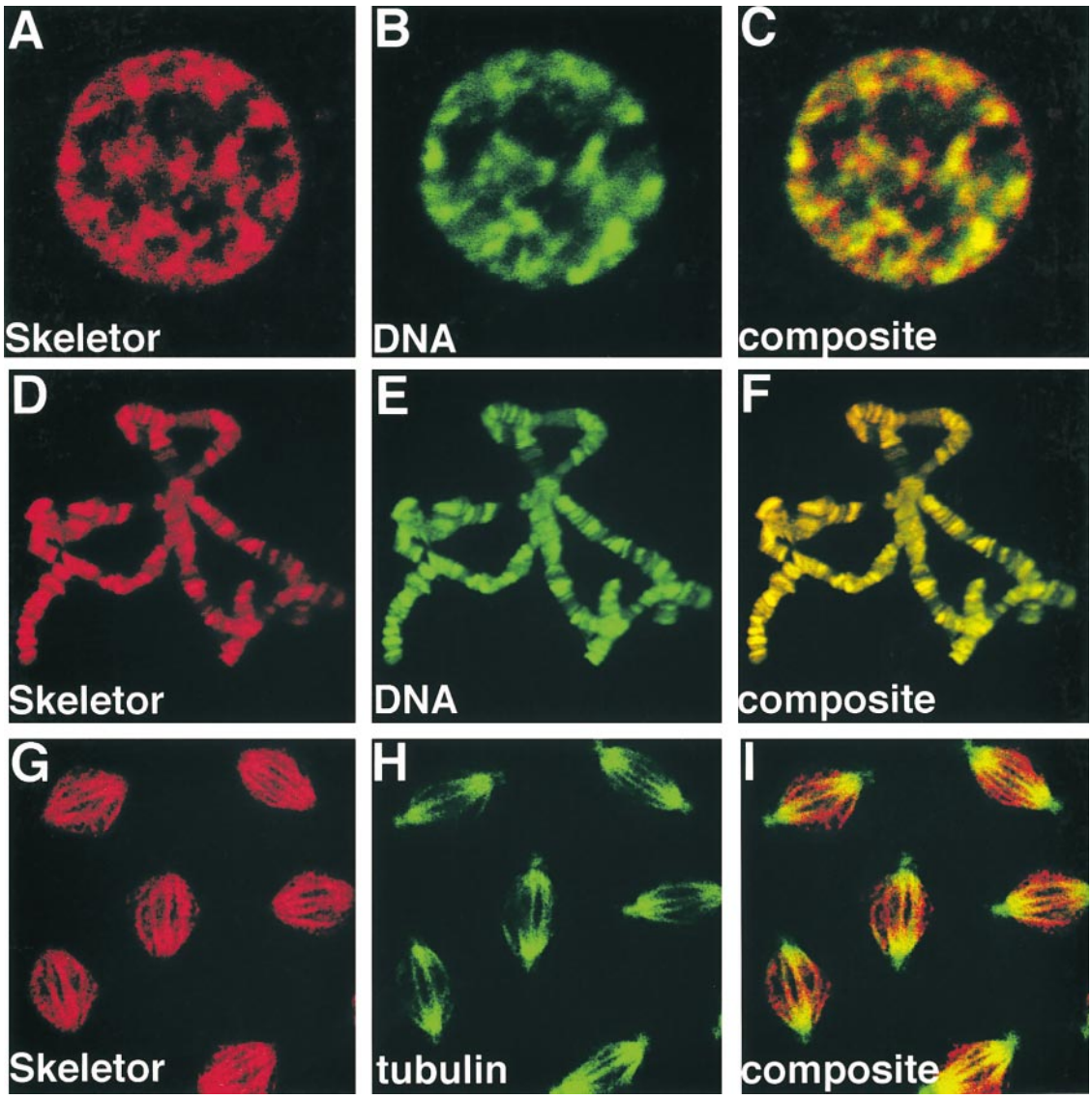

Figure 3. Skeletor associates with chromosomes at interphase, but is coaligned with the microtubule spindle at metaphase. (A–C) Confocal imaging of an interphase embryonic nucleus reveals that the skeletor mAb1A1 stains a fibrous structure (A) similar in appearance to Hoechst staining of the DNA (B). The composite images (C) show extensive overlap of skeletor labeling with that of the chromosomes. (D–F) Larval polytene squashes stained with mAb1A1 (D) show a banded pattern of staining that overlaps with the densely stained Hoechst bands (E), as determined by the predominantly yellow banding pattern observed in the composite image (F). (G–I) Confocal section of *Drosophila* metaphase spindles double labeled with mAb1A1 (G) and α-tubulin antibody (H). The composite image of mAb1A1 (G) and α-tubulin staining (H) is shown in (I). mAb1A1 clearly labels a true fusiform spindle structure that is colocalized with the microtubule spindle, except for the centrosomes.

gether with Hoechst to visualize the chromosomes. Fig. 4 A shows that at late prophase, when the microtubules have not yet entered the nuclear space (Kellogg et al., 1988), the skeletor spindle is already aligned within the nucleus. During metaphase, the two spindles are coaligned, though the skeletor spindle appears broader than the microtubule spindle. The skeletor spindle continues to extend between the two poles at anaphase as the chromosomes segregate (Fig. 4 C), and at telophase midbody formation of the microtubules is found to align with the central portion of the skeletor spindle (Fig. 4 A). At this stage, both the chromosomes and the skeletor spindle have begun decondensing at the poles as skeletor reassociates with the chromosomes. Fig. 4 B shows that skeletor begins to dissociate from its chromosomal colocalization during prophase and forms an observable spindle by late prophase. At this time, though the nuclear lamina has deformed at the centrosomal positions where an abundance of microtubules begin to aggregate (Paddy et al., 1996), it is still intact. During prophase, skeletor is clearly associated with the nuclear lamina (Fig. 4 B, yellow in the composite image). Quadruple labeling of late prophase embryonic nuclei (Fig. 5) allows simultaneous imaging of skeletor, lamin, tubulin, and the DNA. Whereas the skeletor spindle has formed within the nuclear space encircled by the now deforming nuclear lamina, the microtubules have not yet established a spindle structure. By metaphase, the skeletor spindle is fully formed, chromo-

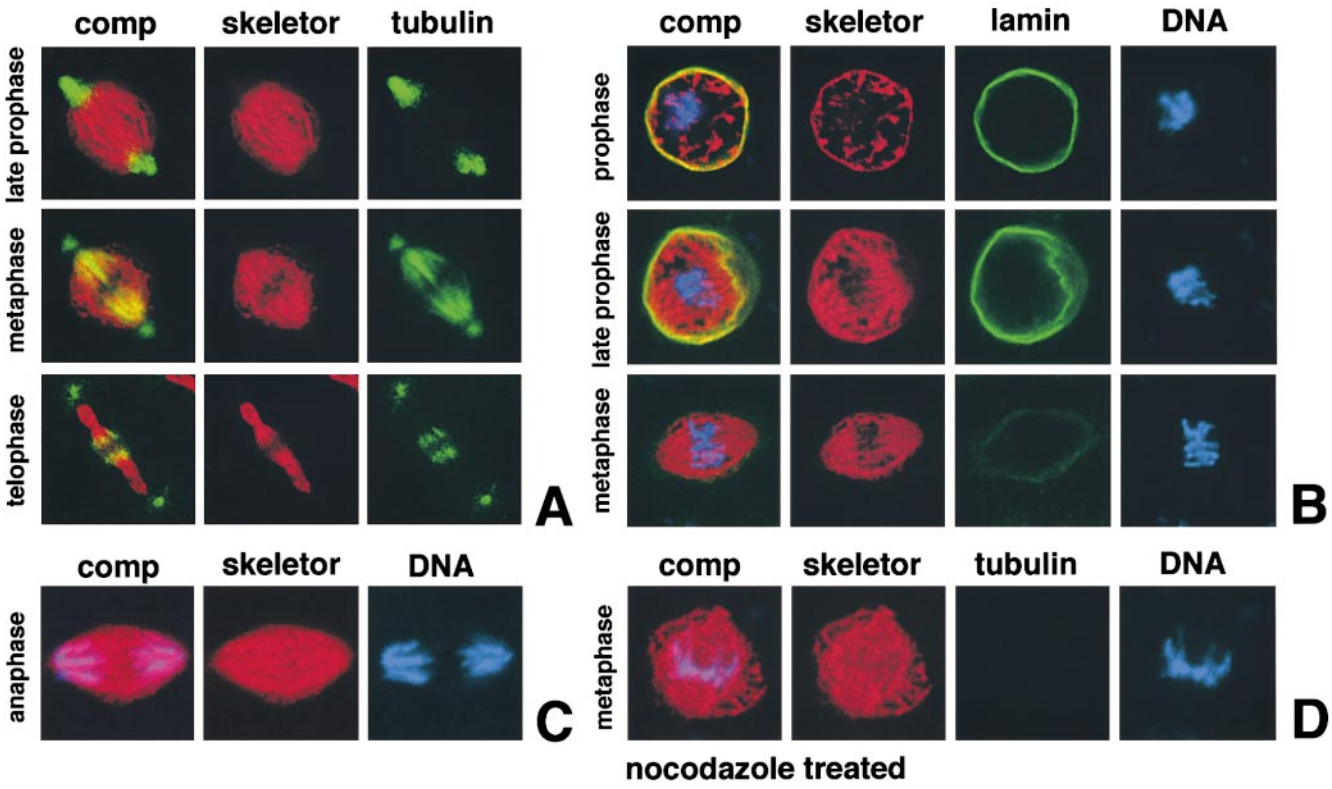

Figure 4. Skeletor spindle formation begins before microtubule entry into the nucleus or nuclear lamina breakdown. (A) Double labelings with mAb1A1 to visualize skeletor (red) and anti–α-tubulin to visualize the microtubules (green) show that in late prophase, when the microtubules have not yet entered the nuclear space, the skeletor spindle is already aligned within the nucleus. During metaphase, the two spindles are coaligned, though the skeletor spindle appears broader than the microtubule spindle. During telophase, the chromosomes have segregated and as they decondense, they reassociate with skeletor at the poles. However, the skeletor spindle persists in the central region where midbody formation of the microtubules is found to take place in alignment with the skeletor spindle. (B) Triple labelings using mAb1A1 to visualize skeletor (red), anti-lamin antibody to visualize the nuclear lamina (green), and Hoechst to visualize the DNA (blue) reveal that skeletor dissociates from its chromosomal localization during prophase and forms an observable spindle by late prophase. At this time, though the nuclear lamina has begun to "dimple," it is still intact. During prophase, skeletor is clearly associated with the nuclear envelope (yellow in the composite images [comp]). By metaphase, the skeletor spindle is fully formed, chromosomes have aligned at the metaphase plate, and the nuclear lamina has largely disassembled. (C) The skeletor spindle (red) persists as an intact spindle extending across the metaphase plate as the chromosomes (blue) segregate to the poles. (D) Nocodazole-treated *Drosophila* embryo at metaphase triple labeled with mAb1A1 (red), α-tubulin antibody (green), and Hoechst (DNA in blue). The microtubule spindles have completely depolymerized, as indicated by the absence of microtubule labeling (green). The mAb1A1-labeled spindle (red) is still intact, albeit slightly deformed, demonstrating that this structure persists independent of the microtubule spindle. All images represent confocal images. Dynamic three-dimensional reconstructions of similar labelings to those presented in this figure are available as supplemental material online at http://www.jcb.org/cgi/content/full/151/7/1401/DC1.

somes have aligned at the metaphase plate, and the nuclear lamina has largely disassembled (Fig. 4 B). Thus, these results provide evidence that skeletor spindle formation begins before microtubule entry into the nucleus or nuclear lamina breakdown.

To further address the relationship between the skeletor and microtubule spindles, we conducted triple-labeling studies in embryos where microtubules were disassembled by either nocodazole or cold treatment. Fig. 4 D shows an image of a skeletor spindle from a nocodazole-treated embryo arrested at metaphase. There was no detectable tubulin antibody labeling, indicating that the nocodazole treatment resulted in total disassembly of the microtubules (Fig. 4 D, tubulin). However, even in the absence of microtubule spindles, the skeletor spindle remains intact, implying that the existence of the skeletor spindle does not require polymerized microtubules. Nonetheless, we observed in many cases that the skeletor spindle does become somewhat deformed upon microtubule disassembly, suggesting that the skeletor spindle may depend on interactions with microtubules for its correct morphology. Identical results were obtained when spindles were disassembled using cold treatment (data not shown).

Antibody Perturbation of Skeletor Disrupts Embryonic Development

The dynamic staining patterns observed with skeletor antibody suggest that skeletor plays an important role in nuclear structure and function. To directly test whether skeletor is essential for embryonic development, early syncytial embryos (0–30 min) were injected with either anti-skeletor ascites or control ascites, allowed to develop for 2.5 h, fixed, and the nuclei were visualized with Hoechst. Fig. 6, A and B, shows representative embryos injected with anti-skeletor antibody. These embryos had fewer nuclei than the control em-

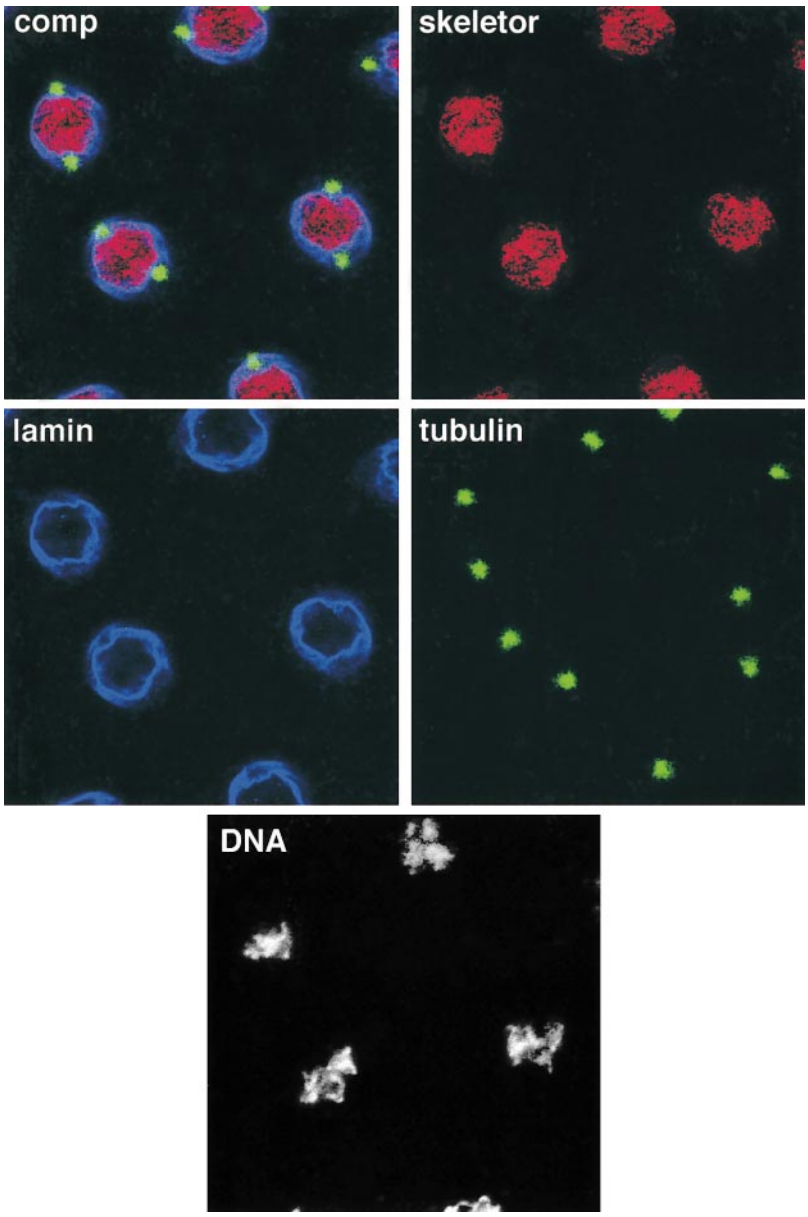

Figure 5. Localization of skeletor, α-tubulin, lamin, and DNA at late prophase in *Drosophila* embryos. Quadruple labelings of prophase nuclei using mAb1A1 to visualize skeletor (red), anti-lamin antibody to visualize the nuclear lamina (blue), anti–α-tubulin antibody to visualize the microtubules (green), and Hoechst to visualize the DNA (white) reveal that the skeletor spindle has initiated formation before nuclear lamina breakdown and before microtubules can be detected within the nuclear space. The composite panel (comp) shows a merged image of the skeletor, lamin, and tubulin channels, all of which were imaged at the same plane. The DNA panel was imaged from a slightly deeper plane of section, which better represents the condensation state of the DNA.

bryos and the Hoechst-labeled DNA appeared fragmented and in various stages of disintegration. This perturbation was highly robust, as 90% of the experimental embryos showed this phenotype (111 out of 124). In contrast, control injections of a monoclonal antibody from a commercially available IgM-containing ascites (MOPC-104E), which does not recognize any *Drosophila* antigens, showed no effect (Fig. 6, C and D) in 89% of the injected animals (107 out of 120). χ^2 analysis indicates that the difference between the control and experimental animals is statistically significant ($P < 0.001$). Similar results were obtained using a control ascites raised in our own laboratory against the lan3-2 leech antigen (Huang et al., 1997) that does not cross-react in *Drosophila* (data not shown). Thus, these results suggest that mAb1A1 has a function blocking effect and can perturb embryonic development, though we do not as yet know whether the observed phenotype is a direct or indirect consequence of blocking skeletor function.

Discussion

Here, we report the cloning and characterization of *Drosophila* skeletor, one of the antigens recognized by the mAb2A (Johansen et al., 1999). The skeletor locus is highly complex, with alternative splicing that gives rise to two mRNAs. The smaller mRNA codes for a cytoplasmic localized protein of 32 kD. The other and larger mRNA has bicistronic coding potential with the skeletor ORF localized downstream and the putative starting methionine followed by an inframe stop codon. At present, we do not know whether skeletor is translated from the indicated methionine and is able to read through the stop codon, or whether some type of frameshift mechanism or use of an alternative start codon is responsible for translation initiation. However, the detection of skeletor with multiple mono- and polyclonal antibodies, which were generated against separate domains of the protein and their identical immunocytochemical labeling of embryonic nuclei, demonstrate that, not withstanding the unconventional organi-

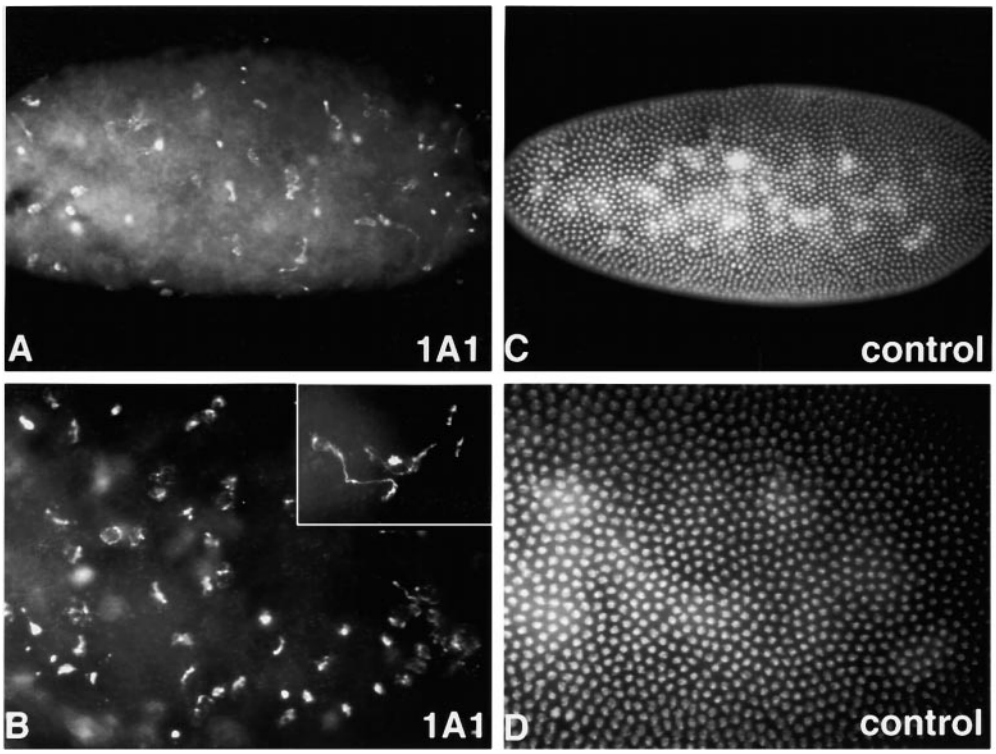

Figure 6. mAb1A1 perturbation analysis of nuclear development in syncytial embryos. The mAb1A1 (A and B) or control IgM antibody (C and D) was injected into early, syncytial stage embryos that were allowed to develop for 2.5 h before fixation, devitellinization, and Hoechst staining. (A) Experimental embryo injected with mAb1A1 shows fewer nuclei that are disorganized and mislocalized. (B) At higher magnification, nuclei in mAb1A1-injected embryos show lack of nuclear structure and are in various stages of fragmentation (insert). (C) Embryo injected with control antibody develops normally and appears wild-type in its Hoechst-staining pattern. (D) At higher magnification, nuclei from control-injected embryos are synchronized and show normal nuclear morphology.

zation of the skeletor mRNA, the skeletor ORF is in fact translated. Skeletor is a novel protein of 81 kD, which, apart from a bipartite nuclear localization signal, is without functional domains identified in other proteins.

Labeling of embryonic nuclei in various stages of the cell cycle demonstrated that skeletor is associated with the chromosomes at interphase, but at prophase, it redistributes into a true fusiform spindle structure that precedes microtubule spindle formation, and that this spindle can exist independently of microtubules. Our interpretation of this dynamic redistribution is summarized and diagrammed in the model in Fig. 7. At interphase, skeletor is localized to the chromosomes in a staining pattern overlapping with that of Hoechst-labeled heterochromatin. However, during prophase, as the chromosomes start to condense, skeletor redistributes from the chromosomes and into a fibrous meshwork, which aligns to form a distinct spindle structure at late prophase. At this stage, nucleated microtubules have been accumulating around the centrosomes, but have not yet invaded the nuclear space as the nuclear lamina is still intact. During prophase, skeletor is also detected colocalizing with the nuclear envelope. At metaphase, the nuclear envelope has broken down at the poles and microtubule spindle fibers coalign with the skeletor-defined spindle, with the chromosomes positioned at the metaphase plate. Remnants of the nuclear lamina are still associated with the outer parts of the skeletor spindle. During anaphase, the skeletor spindle narrows, but remains stable and intact as the chromosomes segregate. At telophase, the chromosomes start to decondense and reassociate with skeletor where the two daughter nuclei are forming while skeletor still defines a spindle in the midregion. Microtubules associate with the skeletor spindle in this region, providing a basis for tubulin midbody formation and alignment.

At present, we do not know whether skeletor itself forms the observed spindle or whether it associates with other macromolecules that provide the actual structural elements. However, since skeletor does not possess any known protein motifs with such a function, it is likely that the skeletor antibody-labeling pattern reflects the formation of a macromolecular complex constituted by several nuclear components. We further propose that this macromolecular complex, of which skeletor is a member, constitutes a spindle matrix. A spindle matrix has been hypothesized to provide a more or less stationary substrate that anchors motor molecules during force production and microtubule sliding (Pickett-Heaps et al., 1997). Such a matrix would also have the properties of helping to organize and stabilize the microtubule spindle. Clearly, the formation of the skeletor-defined spindle before nuclear lamina breakdown suggests it may function as a guide for microtubule extension towards the metaphase plate. However, the fact that the skeletor-defined spindle matrix is aligned with the centrosomes implies the existence of a mechanism that coordinates this alignment with centrosome positioning across the nuclear membrane. The finding that the skeletor-defined spindle matrix maintains its fusiform spindle structure from end to end across the metaphase plate during anaphase when the chromosomes segregate makes it an ideal substrate for providing structural support stabilizing microtubules and for counterbalancing force production. The identification and characterization of skeletor is the first direct molecular evidence for the existence of a complete spindle matrix that forms within the nucleus. The NuMA (nuclear mitotic apparatus) protein, another proposed component of the spindle matrix, is located to the spindle poles at metaphase, assisting in stabilizing and focusing microtubules in the region near the

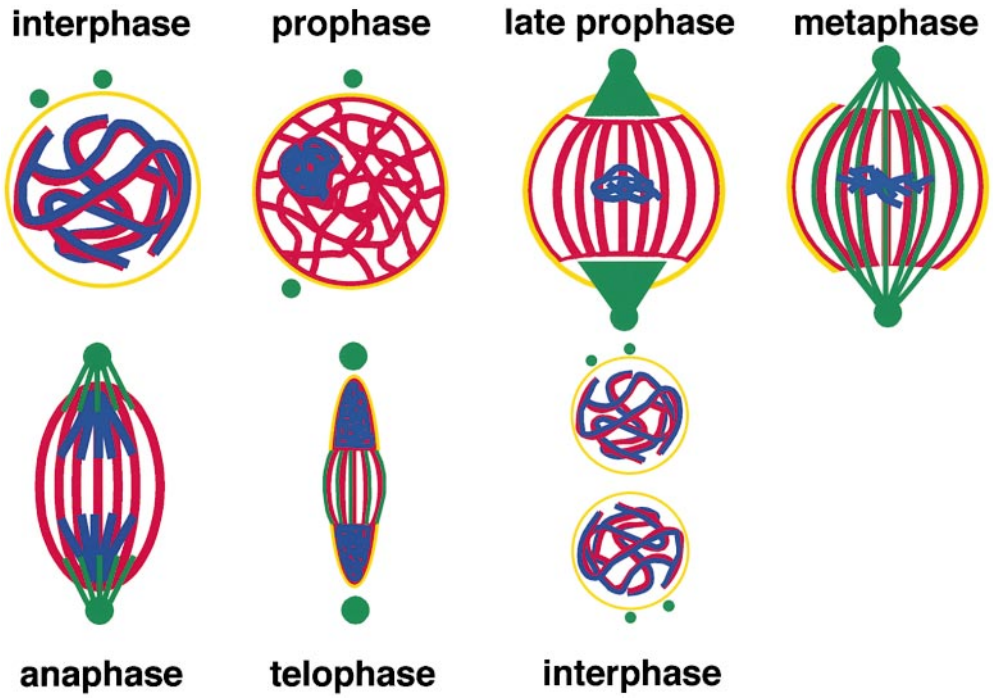

Figure 7. Diagram of skeletor redistribution during mitosis. Skeletor is indicated in red, heterochromatin in blue, centrosomes and microtubules in green, and the nuclear lamina in yellow.

centrosomes (Merdes et al., 1996; Dionne et al., 1999). CP60 and CP190, two proteins that shuttle between the centrosomes and the nucleus (Kellogg et al., 1995; Oegema et al., 1995), also localize in a fibrous pattern that persists into mitosis (Oegema et al., 1997). The redistribution of CP190 from centrosomes into the nucleus that occurs during prophase could provide a mechanism by which the skeletor spindle becomes aligned with the centrosomes, despite the absence of microtubules in the nucleus. Skeletor is likely to play an important role in nuclear function as antibody perturbation experiments in *Drosophila* embryos lead to nuclear fragmentation and reduced mitotic divisions. However, these experiments do not address whether this phenotype is a result of skeletor having a role in spindle assembly and/or function, or whether it may have additional roles in maintaining chromatin structure as its chromosomal localization during interphase may imply. The future isolation and characterization of mutants defective in skeletor in *Drosophila* promises to resolve these questions and to provide further insights into the function of this protein and the spindle matrix.

We wish to thank Anna Yeung for excellent technical assistance and Drs. P. Wilson and A. Forer for help with the initial confocal analysis.

This work was supported by a National Science Foundation (NSF) grant MCB-9600587 (K.M. Johansen), by an NSF Training Grant DIR-9113595 graduate fellowship (D.L. Walker), and by a Fung graduate fellowship (Y. Jin).

Submitted: 19 September 2000
Revised: 13 November 2000
Accepted: 14 November 2000

References

Adams, M.D., S.E. Celniker, R.A. Holt, C.A. Evans, J.D. Gocayne, P.G. Amanatides, S.E. Scherer, P.W. Li, R.A. Hoskins, R.F. Galle, et al. 2000. The genome sequence of *Drosophila melanogaster*. *Science.* 287:2185–2195.

Baek, K.-H., and L. Ambrosio. 1995. An efficient method for microinjection of mRNA into *Drosophila* embryos. *Biotechniques.* 17:1024–1026.

Casiano, C.A., G. Landberg, R.L. Ochs, and E.M. Tan. 1993. Autoantibodies to a novel cell cycle-regulated protein that accumulates in the nuclear matrix during S phase and is localized in the kinetochores and spindle midzone during mitosis. *J. Cell Sci.* 106:1045–1056.

Compton, D.A., I. Szilak, and D.W. Cleveland. 1992. Primary structure of NuMA, an intranuclear protein that defines a novel pathway for segregation of proteins at mitosis. *J. Cell Biol.* 116:1395–1408.

Cooke, C.A., M.S. Heck, and W.C. Earnshaw. 1987. The inner centromere protein (INCENP) antigens: movement from inner centromere to midbody during mitosis. *J. Cell Biol.* 105:2053–2067.

Dionne, M.A., L. Howard, and D.A. Compton. 1999. NuMA is a component of an insoluble matrix at mitotic spindle poles. *Cell Motil. Cytoskeleton.* 42:189–203.

Earnshaw, W.C., and C.A. Cooke. 1991. Analysis of the distribution of the INCENPs throughout mitosis reveals the existence of a pathway of structural change in the chromosomes during metaphase, and the early events in cleavage furrow formation. *J. Cell Sci.* 98:443–461.

Elgin, S.C.R., and L.E. Hood. 1973. Chromosomal proteins of *Drosophila* embryos. *Biochemistry.* 12:4984–4991.

Forer, A., T. Spurck, and J.D. Pickett-Heaps. 1997. Ultraviolet microbeam irradiations of spindle fibres in crane-fly spermatocytes and newt epithelial cells: resolution of previously conflicting observations. *Protoplasma.* 197:230–240.

Gard, D.L. 1992. Microtubule organization during maturation of *Xenopus* oocytes: assembly and rotation of the meiotic spindles. *Dev. Biol.* 151:516–530.

Goldstein, L.S., R.A. Laymon, and J.R. McIntosh. 1986. A microtubule-associated protein in *Drosophila melanogaster*: identification, characterization, and isolation of coding sequences. *J. Cell Biol.* 102:2076–2087.

Harlow, E., and E. Lane. 1988. Antibodies: A Laboratory Manual. Cold Spring Harbor Laboratory Press, Cold Spring Harbor, NY. 726 pp.

Huang, Y., J. Jellies, K.M. Johansen, and J. Johansen. 1997. Differential glycosylation of tractin and LeechCAM, two novel Ig superfamily members, regulates neurite extension and fascicle formation. *J. Cell Biol.* 138:143–157.

Jin, Y., Y. Wang, D.L. Walker, H. Dong, C. Conley, J. Johansen, and K.M. Johansen. 1999. JIL-1: a novel chromosomal tandem kinase implicated in transcriptional regulation in *Drosophila*. *Mol. Cell.* 4:129–135.

Johansen, K.M. 1996. Dynamic remodeling of nuclear architecture during the cell cycle. *J. Cell. Biochem.* 60:289–296.

Johansen, K.M., J. Johansen, K.-H. Baek, and Y. Jin. 1996. Remodeling of nuclear architecture during the cell cycle in *Drosophila* embryos. *J. Cell. Biochem*. 63:268–279.

Johansen, K.M., J. Johansen, Y. Jin, D.L. Walker, D. Wang, and Y. Wang. 1999. Chromatin structure and nuclear remodeling. *Crit. Rev. Eukaryot. Gene Expr.* 9:267–277.

Kellogg, D.R., T.J. Mitchison, and B.M. Alberts. 1988. Behavior of microtubules and actin filaments in living *Drosophila* embryos. *Development.* 103: 675–686.

Kellogg, D.R., K. Oegema, J. Raff, K. Schneider, and B.M. Alberts. 1995. CP60: a microtubule-associated protein that is localized to the centrosome in a cell cycle-specific manner. *Mol. Biol. Cell.* 6:1673–1684.

Leslie, R.J., R.B. Hird, L. Wilson, J.R. McIntosh, and J.M. Scholey. 1987. Kinesin is associated with a nonmicrotubule component of sea urchin mitotic

spindles. *Proc. Natl. Acad. Sci. USA.* 84:2771–2775.
Lydersen, B.K., and D.E. Pettijohn. 1980. Human specific nuclear protein that associates with the polar region of the mitotic apparatus: distribution in a human/hamster hybrid cell. *Cell.* 22:489–499.
Mackay, A.M., D.M. Eckley, C. Chue, and W.C. Earnshaw. 1993. Molecular analysis of the INCENPs (inner centromere proteins): separate domains are required for association with microtubules during interphase and with the central spindle during anaphase. *J. Cell Biol.* 123:373–385.
Merdes, A., K. Ramyar, J.D. Vechio, and D.W. Cleveland. 1996. A complex of NuMA and cytoplasmic dynein is essential for mitotic spindle assembly. *Cell.* 87:447–458.
Mitchison, T.J. 1989. Polewards microtubule flux in the mitotic spindle: evidence from photoactivation of fluorescence. *J. Cell Biol.* 109:637–652.
Mitchison, T., and J. Sedat. 1983. Localization of antibody determinants to whole *Drosophila* embryos. *Dev. Biol.* 99:261–264.
Oegema, K., W.G. Whitfield, and B.M. Alberts. 1995. The cell cycle–dependent localization of the CP190 centrosomal protein is determined by the coordinate action of two separable domains. *J. Cell Biol.* 131:1261–1273.
Oegema, K., W.F. Marshal, J.W. Sedat, and B.M. Alberts. 1997. Two proteins that cycle asynchronously between centrosomes and nuclear structures: *Drosophila* CP60 and CP90. *J. Cell Sci.* 110:1573–1583.
Paddy, M.R., H. Saumweber, D.A. Agard, and J.W. Sedat. 1996. Time-resolved, in vivo studies of mitotic spindle formation and nuclear lamina breakdown in *Drosophila* early embryos. *J. Cell Sci.* 109:591–607.
Pankov, R., M. Lemieux, and R. Hancock. 1990. An antigen located in the kinetochore region in metaphase and on polar microtubule ends in the midbody region in anaphase, characterized using a monoclonal antibody. *Chromosoma.* 99:95–101.
Pickett-Heaps, J.D., A. Forer, and T. Spurck. 1997. Traction fiber: toward a "tensegral" model of the spindle. *Cell Motil. Cytoskeleton.* 37:1–6.
Reinhardt, A., and T. Hubbard. 1998. Using neural networks for prediction of the subcellular location of proteins. *Nucleic Acids Res.* 26:2230–2236.
Robbins, J., S.M. Dilworth, R.A. Laskey, and C. Dingwall. 1991. Two interdependent basic domains in nucleoplasmin nuclear targeting sequence: identification of a class of bipartite nuclear targeting sequence. *Cell.* 64:615–623.
Roberts, D.B. 1986. *Drosophila*: A Practical Approach. IRL Press at Oxford University, UK. 295 pp.
Sawin, K.E., and T.J. Mitchison. 1991. Poleward microtubule flux in mitotic spindles assembled in vitro. *J. Cell Biol.* 112:941–954.
Sawin, K.E., and T.J. Mitchison. 1994. Microtubule flux in mitosis is independent of chromosomes, centrosomes, and antiparallel microtubules. *Mol. Biol. Cell* 5:217–226.
Sambrook, J., E.F. Fritsch, and T. Maniatis. 1989. Molecular Cloning: A Laboratory Manual. Cold Spring Harbor Laboratory Press, Cold Spring Harbor, NY. 545 pp.
Theurkauf, W.E., and R.S. Hawley. 1992. Meiotic spindle assembly in *Drosophila* females: behavior of nonexchange chromosomes and the effects of mutations in the nod kinesin-like protein. *J. Cell Biol.* 116:1167–1180.
Towbin, H., T. Staehelin, and J. Gordon. 1979. Electrophoretic transfer of proteins from polyacrylamide gels to nitrocellulose sheets: procedure and some applications. *Proc. Natl. Acad. Sci. USA.* 9:4350–4354.
Yang, C.H., and M. Snyder. 1992. The nuclear-mitotic apparatus protein is important in the establishment and maintenance of the bipolar mitotic spindle apparatus. *Mol. Biol. Cell.* 3:1259–1267.
Yen, T.J., D.A. Compton, D. Wise, R.P. Zinkowski, B.R. Brinkley, W.C. Earnshaw, and D.W. Cleveland. 1991. CENP-E, a novel human centromere-associated protein required for progression from metaphase to anaphase. *EMBO (Eur. Mol. Biol. Organ.) J.* 10:1245–1254.
Zhang, D., and R.B. Nicklas. 1995a. Chromosomes initiate spindle assembly upon experimental dissolution of the nuclear envelope in grasshopper spermatocytes. *J. Cell Biol.* 131:1125–1131.
Zhang, D., and R.B. Nicklas. 1995b. The impact of chromosomes and centrosomes on spindle assembly as observed in living cells. *J. Cell Biol.* 129: 1287–1300.
Zink, B., and R. Paro. 1989. In vivo binding pattern of a trans-regulator of homoeotic genes in *Drosophila melanogaster*. *Nature.* 337:468–471.